Plasma Chem Plasma Process (2008) 28:535–551
DOI 10.1007/s11090-008-9136-0

ORIGINAL PAPER

Influence of Plasma Treatments on the Hemocompatibility of PET and PET + TiO_2 Films

Ionut Topala · Nicoleta Dumitrascu · Valentin Pohoata

Received: 11 July 2006 / Accepted: 20 October 2006 / Published online: 24 June 2008

Abstract A dielectric barrier discharge (DBD) in helium was used to ameliorate the interface between the blood and the surface of polymeric implants: polyethylene terephthalate (PET) and PET with titanium oxide (PET + TiO_2). A higher crystallinity degree was found for the DBD treated samples. The wettability of polymers was improved after the treatment. The chemical composition, analyzed by infrared spectroscopy was preserved during the DBD treatment. The surface modifications have been correlated with polymers hemocompatibility. Concerning the polymer surface–blood interaction, the treatment induced a decrease of the interfacial tension between the blood components and the treated surfaces. The in vitro tests of hemocompatibility showed no perturbation in the blood composition when the polymer samples are present in the blood volume. An interesting result is related to the whole blood clotting time that shows a dramatic increase on the treated surfaces. Moreover, the coagulation kinetics on the treated surfaces is modified.

Keywords Blood–material interface · Dielectric barrier discharge · Hemocompatibility · Polymers · Surface modification

Introduction

The polymers are nowadays used in many medical devices and therefore have a direct contact with the blood, as in the heart valves and artificial heart, vascular prostheses, blood pumps, dialysis membranes, blood bags, etc. One of the common hazards caused by the contact between the implants and the blood is the thrombus formation and the surface properties are the key in controlling the coagulation factors and the thrombogenic effects [1].

Among the large variety of physical and chemical methods used to obtain surfaces with anti-thrombogenic properties, plasma treatments are a convenient and efficient technique

I. Topala (✉) · N. Dumitrascu · V. Pohoata
Plasma Physics Laboratory, Faculty of Physics, Alexandru Ioan Cuza University,
Blvd. Carol I, No. 11, 700506 Iasi, Romania
e-mail: itopala@plasma.uaic.ro

[2–4]. Generally, the plasma treatments of polymers improve the wettability and adhesion properties, enhance the crystallinity degree, create a high density of functional groups onto the surface and an increased polarity, etc. Due to these effects, the plasma processing may be used to improve the biocompatibility and the hemocompatibility, or as a preliminary treatment in many other techniques of immobilization of biological active molecules (enzymes, drugs, etc.) onto the polymeric substrates [5, 6].

In our experiments a dielectric barrier discharge (DBD) in helium at atmospheric pressure was used as a suitable and efficient technique to induce surface modifications, with benefic effects in the medical applications. By comparison with the classical low pressure plasma processing, the DBD technique has several advantages, as working at atmospheric pressure in various geometries, inducing homogenous and efficient treatment due to the chemical active species present in the volume of plasma and near the surface, exposure of the sample to minimum thermal stress, low cost and easy to implement in industrial processing [7, 8].

From the wide range of synthetic polymers used as materials for human implantation, the polyethylene terephthalate (PET) has a long history, being firstly introduced in medicine in the 1960s as suture fibers and vascular prostheses. PET is a linear polyester with hydrophobic character and low adhesion properties, resistant to hydrolysis, with good stability in biological environments but having moderate biocompatibility [9–11]. In fact most synthetic polymers have poor biocompatibility and one solution in improving it is to create a hybrid material, such as a composite organic/inorganic, with properties resulting from a combination between those of polymers and those of inorganic materials. These types of composites are often used in orthopedic implants, many new applications in the medical domain being also expected. One of the inorganic compounds with biocompatibility and hemocompatibility properties is the titanium oxide (TiO_2), a hydrophilic additive, with resistance to corrosion and having photocatalytic effects [12]. A few percents of TiO_2 additives in the PET matrix can improve the mechanical, physical and chemical properties of interest in the medical domain, the composites based on polymer/TiO_2 being used in orthopedic surgery and drug delivery systems [13, 14].

The effects of DBD treatments on the PET and PET + TiO_2 films have been analyzed and correlated with the surface properties implied in the hemocompatibility. Thus, the surface morphology was investigated by scanning electron microscopy (SEM), the energetic surface characteristics were defined using contact angle measurements, the crystallinity by X-ray diffraction (XRD) and the chemical structure by Attenuated Total Reflection Fourier Transform Infrared (ATR-FTIR) spectroscopy. The hemocompatibility of the surfaces was analyzed by specific in vitro tests and its relation with the surface properties is also discussed.

Experimental

Materials and Surface Treatments

The samples of PET (transparent films) and PET + pigments of TiO_2 (opaque films) (Terom SA, Iasi, Romania), 0.150 mm thickness, were cleaned with ethanol to remove organic contaminants and dried at room temperature.

The DBD was produced in a Teflon nozzle at atmospheric pressure, with a perforated metal disc as high voltage electrode through which helium was flowing, with 0.15 l/min flow rate. Details about the experimental arrangement were presented elsewhere [8].

Helium was selected due to its effects on the polymeric surfaces, as a low degradation and high crosslinking agent, moreover as a gas which stabilizes the glow discharges at atmospheric pressure in comparison with other gases [15].

The polymer sample was fixed on a glass slide placed on top of the ground electrode, the DBD plasma jet spreading on the dielectric surface. This experimental arrangement generated a DBD in the filamentary mode, controlled by voltage and current measurements and also by optical emission spectroscopy [8]. The treatment duration was 10 s.

Surface Analysis

The surface morphology of the polymer films was investigated by scanning electron microscopy (SEM), using a S-4500 Hitachi scanning electron microscope, with 8 kV acceleration voltage and various magnifications (×2.50 K, ×25.0 K). The samples were coated by sputtering with a platinum layer.

The surface energetic characterization and the interfacial tension estimation between the surface and the biological fluids (fibrinogen, immunoglobulin G, albumin) were performed using contact angle measurements. The sessile drop method was used, with distilled water and formamide as test liquids to calculate the surface energy and its polar and dispersive component.

In Table 1 the energetic characteristics (polar and dispersive components of the surface energy) of the biological liquids are listed. Table 2 presents the same characteristics for the PET and PET + TiO_2 films, calculated and communicated in a previous paper [8]. The polar part of the PET + TiO_2 surface energy is higher by comparison with the PET samples, probably due to the presence of TiO_2 particles in the polymer matrix.

The interfacial tension between the polymer surface and the biological liquids was calculated as [16]

$$\gamma_{SL} = \left[\sqrt{\gamma_{LV}^{p}} - \sqrt{\gamma_{SV}^{p}}\right]^2 + \left[\sqrt{\gamma_{LV}^{d}} - \sqrt{\gamma_{SV}^{d}}\right]^2 \quad (1)$$

where γ_{LV}^{p}, γ_{LV}^{d}, γ_{SV}^{p} and γ_{SV}^{d} are the polar and disperse components of the surface energy.

The contact angle measurements were made in controlled conditions of room temperature and humidity, at different intervals after the DBD treatment (1 h, 1 day, 15 days and 30 days).

The crystalline structure of the polymer films was investigated by XRD using a DRON 2.0 diffractometer with Co K_α radiation ($\lambda = 1.7889$ Å) and the diffraction patterns were fitted with Lorentz type functions. The characteristics corresponding to the diffraction peak (100) were used for the calculations. The variations in the polymer crystallinity were evaluated from the ratio of diffraction peak areas, before and after the plasma treatment.

Table 1 The surface energy of water, blood and plasma proteins [17, 18]

Biological liquids	γ_{LV} (mN/m)	γ_{LV}^{p} (mN/m)	γ_{LV}^{d} (mN/m)
Water	72.80	51.00	21.80
Blood	47.50	36.30	11.20
Fibrinogen	65.00	40.30	24.70
IgG	64.99	35.53	29.46
Albumin	65.00	33.62	31.38

Table 2 The surface energy of polymer samples

Sample	γ_{SV} (mN/m)	γ_{SV}^{p} (mN/m)	γ_{SV}^{d} (mN/m)
Untreated PET	43.27	3.91	39.36
Treated PET	60.46	35.14	25.32
Untreated PET + TiO_2	42.39	15.52	26.87
Treated PET + TiO_2	63.64	41.20	22.44

The crystals size, $D_{(hkl)}$, in the perpendicular direction to the planes family (*hkl*) was calculated using the Scherrer equation [19]

$$D_{(hkl)} = \frac{\lambda}{\beta \cos \theta} \tag{2}$$

and the lattice spacing d using the Bragg equation

$$d = \frac{\lambda}{2 \sin \theta} \tag{3}$$

where λ is the radiation wavelength, β the full width at the half maximum and θ the Bragg's angle.

The ATR-FTIR spectroscopy was performed using a FTIR spectrometer Nicolet Impact 4000, with Smart Golden Gate Single Reflection Diamond as internal reflection element, working in the range 4000–400 cm^{-1}. 64 scans of each sample were taken with 2 cm^{-1} resolution, under the same conditions of room temperature and humidity as for the contact angle measurements.

The area of the 1370 and 1340 cm^{-1} bands was considered to be proportional to the amount of *gauche* and *trans* conformers in PET and PET + TiO_2 samples, respectively. In order to eliminate the artifacts of the ATR technique, like irreproducible optical contact between the sample and the internal reflection element, the absorbance values were normalized to the absorbance of the 1408 cm^{-1} band. The adsorption bands were fitted with Gauss functions, and the values of the integrated area were used to estimate sample crystallinity [20, 21].

Tests of Hemocompatibility

Fresh human blood from healthy, non-medicated and young donors was used and each experiment was made in static conditions, for three different surfaces, i.e. glass (control), untreated and treated polymer surfaces. The work was performed under sterile conditions, keeping constant the area of samples, the temperature and the blood volume. Every test used blood from one human subject and was repeated 5 times, the values reported being averaged over all measured values.

Blood Formula

The samples (1 × 1.5 cm^2) were introduced into test tubes containing 3 ml of fresh vein blood with 60 µl EDTA K3 (7.5%) (Monoject, Sherwood Medical, US), and incubated at 37°C for 30 min. The blood count was performed using a hematology analyzer type ABX MICROS-18 (Horiba ABX International, France). Three tubes were used, one as the

control and two others for the untreated and treated sample, respectively, ensuring the total contact, on both faces, between the blood and the films.

Whole Blood Clotting Time (WBCT)

The blood collected from a punctured finger was deposited as a small drop (0.1 ml) onto each sample (glass, untreated and treated polymer surface) and incubated at 37°C in a constant temperature bath. The clotting time was recorded by manually deepening a stainless-steel needle into the drop to detect any fibrin formation. The time of detection of the first fibrin filament adherent to the needle was considered the coagulation time.

Hemolysis Test

The coagulation process of whole blood onto polymer surfaces was also studied using a spectrophotometric method. 20 samples were used, 5 corresponding to the untreated PET, 5 to the untreated PET + TiO_2 samples and 10 corresponding to the treated ones. A fresh blood drop (0.1 ml) was placed onto each surface, untreated and treated sample and also on the glass, as control surface. Every 10 min, until 50 min in total, the surfaces were washed with 25 ml distillated water and the solutions were transferred into test tubes and incubated for 5 min at 37°C. The concentration of free hemoglobin dispersed in water was evaluated from the UV–Vis spectra of solutions (Perkin-Elmer Lambda-3 spectrophotometer).

Prothrombin Time (PTT)

The blood (4.5 ml) was collected from human vein into the three test tubes containing 0.5 ml sodium citrate 0.129 M (Improvacuter, Improve, China). One tube was the control and the two others contained the untreated and treated samples (1×1.5 cm^2). After 30 min of incubation at 37°C, the platelet-poor plasma (PPP) was obtained by centrifugation at 5000 rot/min for 10 min. Usually this test is used to study the in vivo activation of coagulation cascade, the samples being exposed to whole blood [22, 23]. A quantity of 100 µl PPP was incubated statically at 37°C for 60 s and 200 µl of Thromborel S reagent (Dade-Behring, Germany) was added. Measurements of the PTT were made using a BFT II coagulation analyzer (Dade-Behring, Australia).

Activated Partial Thromboplastin Time (aPTT)

100 µl of PPP was incubated statically at 37°C for 120 s and activated by addition of 100 µl partial thromboplastin reagent Pathrombin SL (Dade-Behring, Germany). The clotting reaction was initiated by adding 100 µl aqueous $CaCl_2$ solution (0.025 mol/l) and the coagulation time was measured using a BFT II coagulation analyzer.

Results

Surface Morphology

The surfaces analyzed by SEM showed a modified morphology after the DBD treatment. Both the untreated PET and PET + TiO_2 surfaces were relatively smooth, homogenous

and defects-free, without specific morphological aspects as worm-like or ripple-like features (Figs. 1a, 2a). Contrary, the treated films showed a new topography, with a high density of crystallites having dimensions in the 50–70 nm range (Figs. 1b, 2b).

Surface Wettability

The contact angle measurements showed an enhanced wettability of the PET and PET + TiO_2 surfaces after 10 s DBD treatment (Fig. 3). The water contact angle values decreased with almost 54% on the PET and with 45% on the PET + TiO_2 surface for 10 s DBD treatments.

Crystallinity

Figure 4 presents an X-ray diffractogram for untreated PET sample, with a well defined diffraction peak at $2\theta \approx 30.02°$ corresponding to the crystal plane (100) and a second peak at $2\theta \approx 26.58°$, corresponding to the crystal plane (110). Based on formulas (2) and (3)

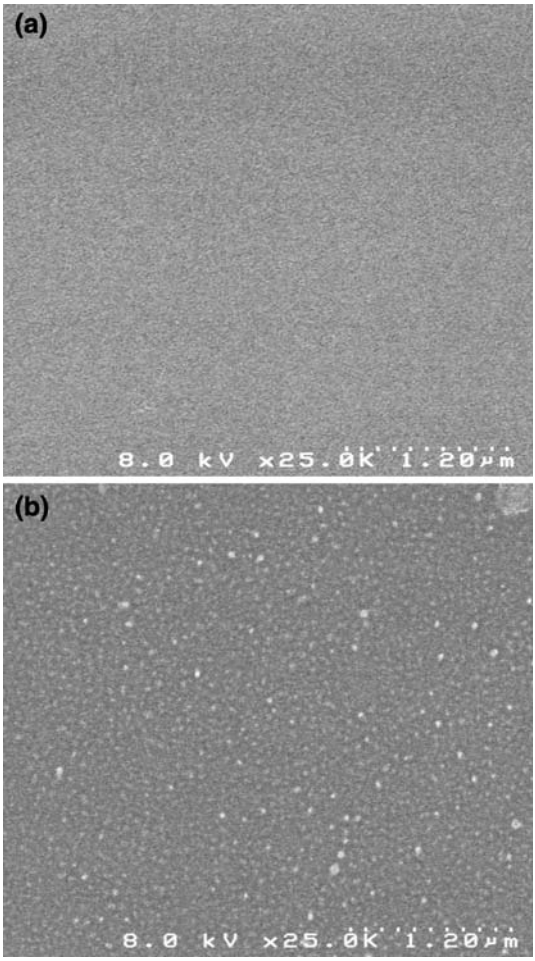

Fig. 1 SEM images of PET films. (**a**) Untreated sample (**b**) 10 s DBD treated sample

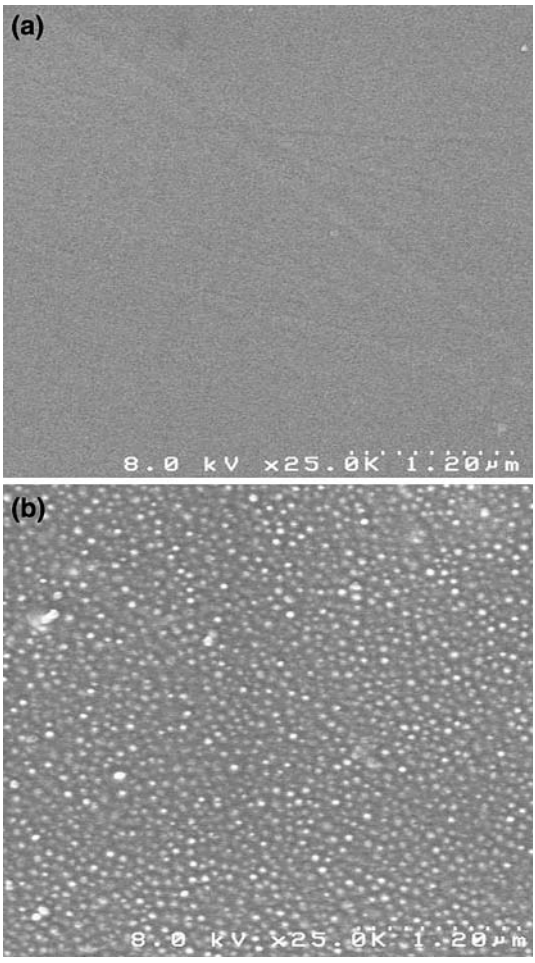

Fig. 2 SEM images of PET + TiO_2 films. (**a**) Untreated sample (**b**) 10 s DBD treated sample

and on the fit analysis results (the full width at the half maximum and 2θ angle), the crystal size ($D_{(100)}$) and the lattice spacing (d) were calculated and the results are listed in Table 3.

Chemical Structure

New adsorption bands were not detected in the ATR-FTIR spectra of DBD treated samples. The intensity of IR bands involved in oxidation reactions remained also unchanged, proving that the overall chemical structure of the polymers was preserved during the treatment. Generally, the polymer chains in PET are arranged in different domains, with a preferential orientation of ethylene glycol residue. Three different regions can be distinguished: a crystalline region, containing only *trans* conformers, an amorphous region, containing *gauche* conformers and a small number of *trans* conformers, and a mesophase region [20, 24, 25]. Figure 5 presents the FTIR spectrum in the 1320–1430 cm^{-1} region for untreated PET. The experimental data in this region were fitted with four bands, two centered at 1408 and 1384 cm^{-1}, corresponding to aromatic CH in plane vibrations, one at 1368 cm^{-1}, corresponding to CH_2 wagging in *gauche* conformers and one at 1340 cm^{-1},

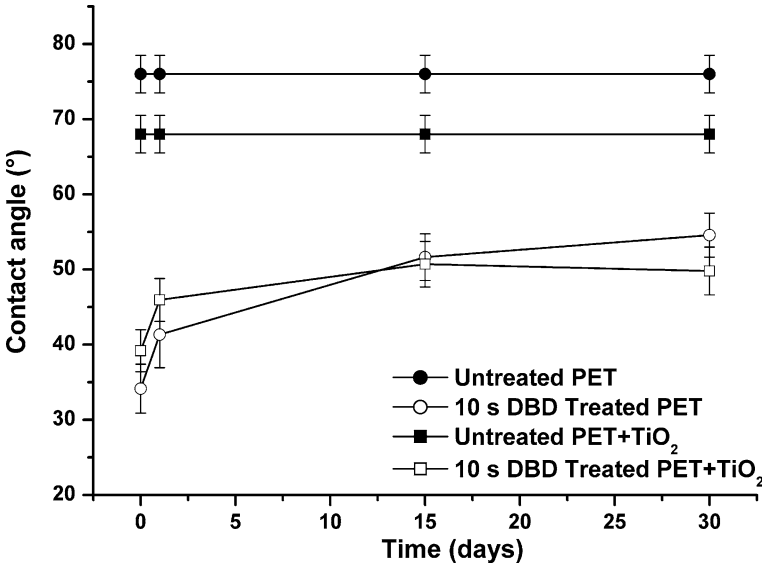

Fig. 3 Water contact angle versus aging time for PET and PET + TiO_2 samples

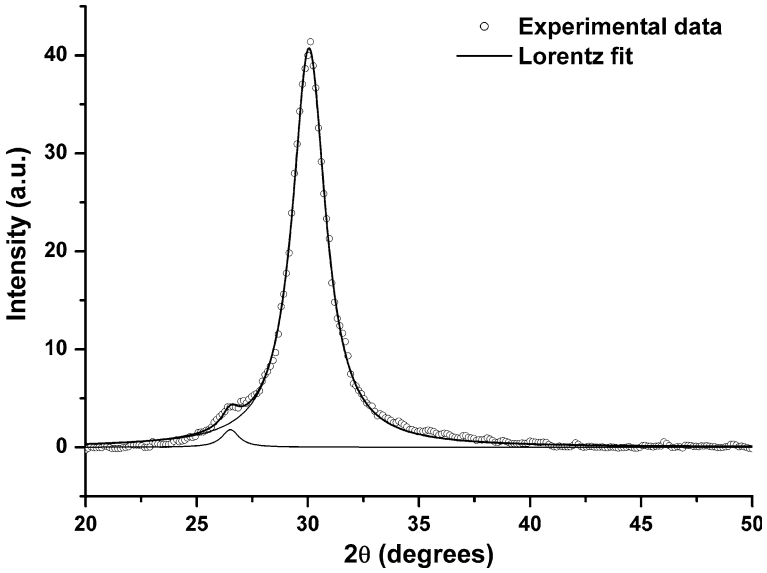

Fig. 4 X-ray diffractogram of the untreated PET surface

corresponding to CH_2 wagging in *trans* conformers. The band areas were used to estimate the variation in the concentration of *trans* and *gauche* conformers. Table 4 lists the ratio between the absorption band areas for *trans* and *gauche* conformers and the area of the reference band.

Table 3 The crystal size $D_{(100)}$ and the lattice spacing *d* for the crystal plane (100)

Sample	$D_{(100)}$ (Å)	d (Å)
Untreated PET	58.54	3.45
Treated PET	59.09	3.44
Untreated PET + TiO_2	60.66	3.46
Treated PET + TiO_2	61.66	3.45

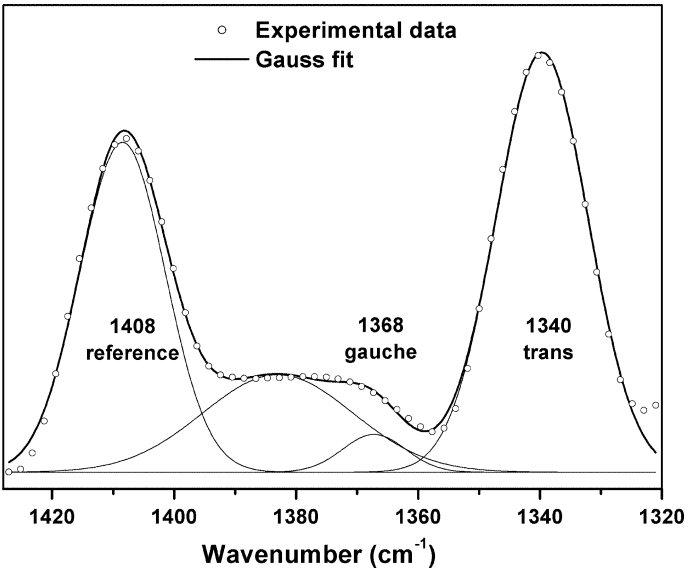

Fig. 5 FTIR spectrum in the 1430–1320 cm^{-1} region and the bands fit for the untreated PET film

Table 4 The ratio between the absorption band areas for *trans* and *gauche* conformers and the area of the reference band

Sample	Trans $area_{1340}$/ $area_{1408}$	Gauche $area_{1370}$/ $area_{1408}$
Untreated PET	1.36	0.08
Treated PET	1.56	0.13
Untreated PET + TiO_2	1.43	0.15
Treated PET + TiO_2	1.49	0.13

Hemocompatibility

Many interactions are possible when the surface of an implant is exposed to the blood, these being expected to perturb the coagulation process at interface. Taking this into account, we analyzed the blood formula, the blood clotting times and the hemolysis process, when the polymeric surface is in the contact with the blood.

Table 5 Blood formula in the presence of polymer samples

Sample	WBC ($\times 10^3$/mm^3)	RBC ($\times 10^6$/mm^3)	PLT ($\times 10^3$/mm^3)
Untreated PET	5.3	5.3	162
Treated PET	5.6	5.0	166
Untreated PET + TiO_2	5.5	4.86	155
Treated PET + TiO_2	5.3	5.12	170
Control	5.6	4.9	184
Normal values	3.5–10.0	3.8–5.8	150–390

Blood Formula

The blood formula in the presence of untreated and treated polymer samples is presented in Table 5. No change in the number and dimensions of white blood cells (WBC), red blood cells (RBC) and platelets (PLT) was found, proving that the blood formula is not perturbed in the presence of the treated polymer surfaces.

Blood Clotting Times

The hemocompatibility of the samples was verified by measurement of the times implicated in the clotting mechanism. The results are summarized in Table 6. Whereas no modifications of PTT and aPTT were found, for the WBCT an increase with 55% on the treated PET and with 88% on the treated PET + TiO_2 surfaces was measured.

Hemolysis Test

The results of the hemolysis test were obtained by adding distilled water on the blood clot formed at the polymer surfaces (protocol described in section "Hemolysis test"). The UV–Vis absorption spectra of these solutions are shown in Figs. 6 and 7. For the untreated samples a hypochromic effect of the hemoglobin absorption bands at 545 and 576 nm is observed (Figs. 6a, 7a). In case of the treated surfaces, even after 50 min, this effect is not so evident, significant absorbencies of hemoglobin bands being recorded (Figs. 6b, 7b).

In order to evaluate the concentration of hemoglobin released in water due to the RBCs lysis the absorbance spectra were integrated from 515 to 600 nm and the results are presented in the Fig. 8. A strong decrease in the band areas is detected in the case of untreated polymer surfaces after 30 min, indicating that at this time the blood clot is strongly linked. Even after 50 min of contact blood–surface, a relative high value of the absorbance in the hemoglobin region is detected and this effect is even more marked in the case of PET + TiO_2 surfaces (Fig. 8b).

Table 6 Clotting times values in the presence on polymer samples

Sample	WBCT (s)	PTT (s)	aPTT (s)
Control	250	13	26.8
Untreated PET	260	12	28.2
Treated PET	410	13.1	26.7
Untreated PET + TiO_2	290	12.9	26.4
Treated PET + TiO_2	530	12.3	25.2

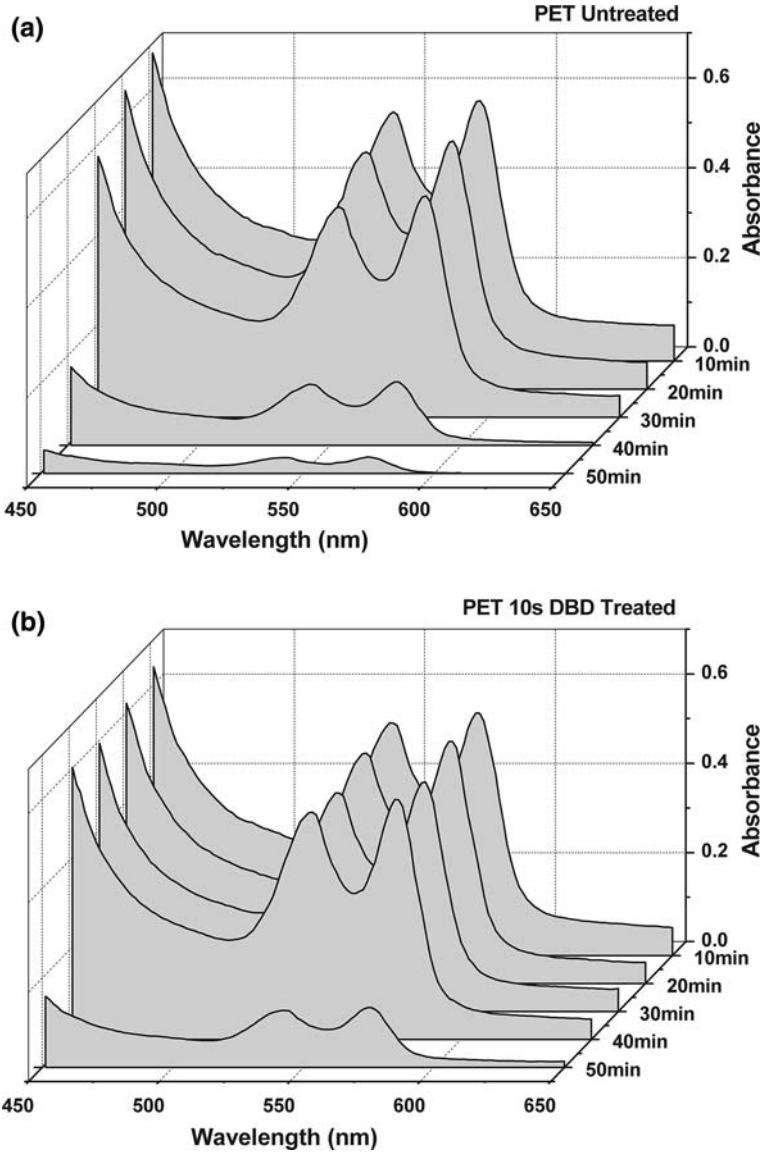

Fig. 6 UV–Vis absorption spectra in the hemolysis test for PET versus time. (**a**) Untreated samples (**b**) 10 s DBD treated samples

Discussion

Due to their energetic components, the plasma treatments can initiate various physico-chemical reactions onto the polymer surface. Moreover, in atmospheric pressure plasmas, due to the high collisions frequency and concentration of excited and ionized species, the reactions take place at a high rate and induce rapid modification of the surface physico-chemical properties. Also, the energetic photons, especially from the ultraviolet domain,

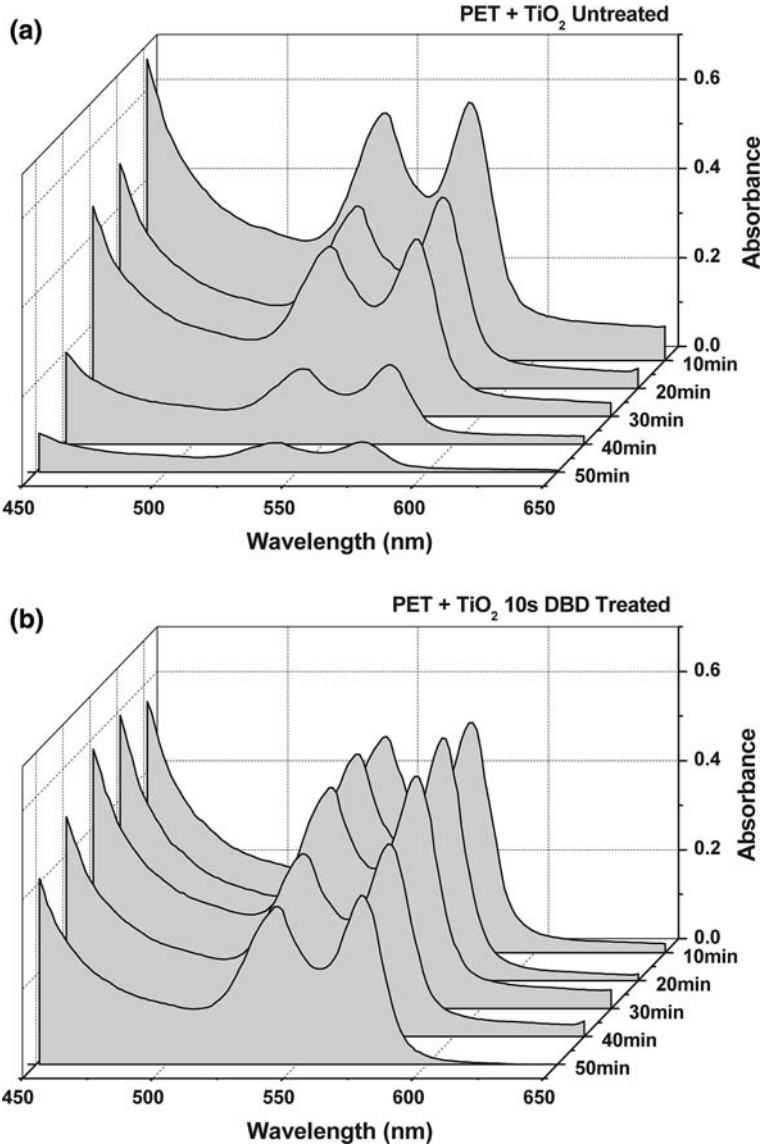

Fig. 7 UV–Vis absorption spectra in the hemolysis test for PET + TiO_2 versus time. (**a**) Untreated samples (**b**) 10 s DBD treated samples

must be taking into account, having an important role in ablation, polymeric chain scission and various chemical reactions [26, 27]. Additionally, due to the low penetration depth of plasma particles in polymer sample, the plasma treatments affect only the surface or/and the near-surface regions.

The surface morphology is very important in the discussion on the biocompatibility and the hemocompatibility. The DBD treated films showed a new morphology, with a high density of crystallites having dimensions in the 50–70 nm range, without a preferential

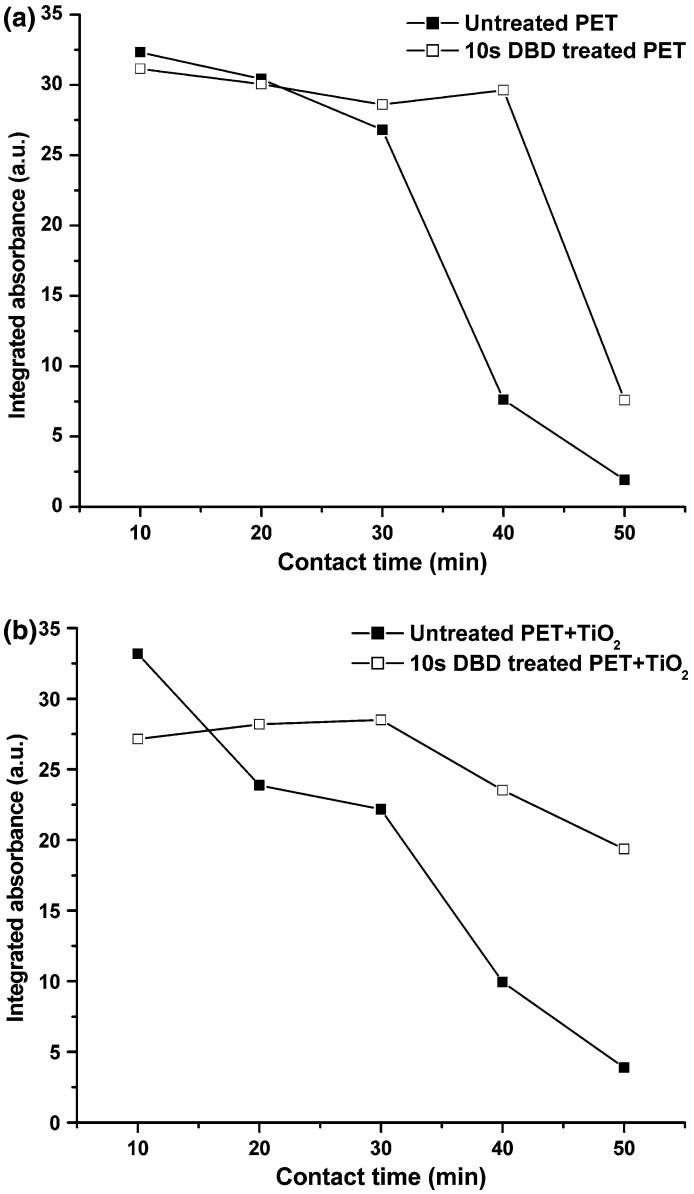

Fig. 8 Integrated absorbance from 515 to 600 nm versus the contact time between whole blood and polymer films. (**a**) PET films (**b**) PET + TiO_2 films

distribution onto the surface. This effect can be explained by the etching of amorphous regions during the treatment, followed by the growth of crystalline domains and the ordering of the molecular chains in the near-surface region of polymer. In particular, this modified morphology could be a favorable for the enhancement of the adhesion properties and the subsequent immobilization of biological active species (drugs, enzymes, cells, etc.) onto the surface.

Generally, the plasma treatments of polymers can improve the wettability and adhesion properties by creating a high density of functional groups onto the surface, an increased polarity, etc. Thus, the contact angle measurements showed an enhanced wettability of the PET and PET + TiO_2 surfaces after the DBD treatment (Fig. 3). After the plasma treatment, in the atmospheric conditions, various physico-chemical processes are possible, including oxidation reactions and polymer chain rearrangements. Thus, during the storage in air at room temperature, the surface wettability, measured by contact angle, showed modification in time, as seen in the Fig. 3. The rapid increase of the contact angle, registered after one day of storage, was followed by stabilization with time, both for the PET and PET + TiO_2 samples, as demonstrated by post-treatment contact angle measurement for 30 days. The better time stabilization observed in the case of PET + TiO_2 samples (Fig. 3) confirms the role of TiO_2 additives in the polymeric matrix as photo stabilizer under atmospheric conditions.

The time stabilization of the surface wettability after the DBD treatments may be correlated with the results on the crystalline structure. A comparison of the X-ray diffractograms of the untreated and treated samples, for both PET and PET + TiO_2, showed no modifications in the shape and the position of the diffraction peaks. Only some changes in their intensity were observed. Thus, for the diffraction peak (100), the ratio of areas treated/untreated was higher than 1, i.e. 1.19 for PET samples and 1.12 for PET + TiO_2, these values indicating a higher degree of crystallinity after the DBD treatments.

The increase of the crystal dimensions ($D_{(100)}$) and the decrease of the lattice spacing (d) (Table 3) confirm that DBD treatments improve the degree of crystallinity, behavior that was also observed in the SEM images (Figs. 1b, 2b). This effect correlates well with the properties of helium plasmas, known to efficiently produce crosslinking reactions [15]. Furthermore, the functional groups based on oxygen and nitrogen, elements inherently present due the atmospheric air entrained in the discharge by the gas flow, can be favorable to the linkages between the adjacent polymeric chains, thus decreasing the molecular mobility at the surface. The crosslinked structure and the lower mobility of polymeric chains may explain the time stability of the surface wettability after the DBD treatment (Fig. 3).

On the other hand, the surface crystallinity and the crystallite size may induce modified adsorption kinetics of proteins and cells onto the surfaces, with effects on the surface hemocompatibility.

During DBD treatment both the configuration and the conformation of the polymer chains may be altered. The FTIR spectra of polymer samples were used to estimate the variation in the concentration of *trans* and *gauche* conformers and a higher amount of *trans* conformers has been found in the DBD treated samples (Table 4). This proves the crystallinity increase in the treated samples, result also confirmed by the SEM images and XRD analysis.

When the surface of an implant is exposed to the blood, many interactions are possible. Plasma proteins adsorption is one of the first events that occur, followed by the cells adherence, affecting the blood formula and its functions. This interaction implies varied processes, such as the simple detachment from the surface, the cell membrane stress accompanied by the alteration of molecular and cellular functions etc., finally leading to cell destruction in blood volume and/or at the surface.

The analysis of the blood formula presented in Table 5 showed no change in the number and dimensions of WBC, RBC and PLT when the treated surface was in contact with the blood.

This represents an important result, taken into account that the contact angles increased after the treatment (Fig. 3) and a higher number of cells would have been therefore expected to adhere onto the treated surface.

On the other hand, a very prolonged clotting time of whole blood onto the treated polymer surfaces was obtained (Table 6) and this result could be correlated with the measurements of the time evolution of the blood clot onto the treated polymer surfaces. Thus, from the UV–Vis absorption spectra of the solutions obtained by adding distillated water onto the blood clot, a decrease of absorbance values for the hemoglobin bands at 545 and 576 nm was observed for the untreated surfaces (Figs. 6a, 7a). In case of the treated surfaces, even after 50 min, we registered significant absorbencies of hemoglobin bands, proving that a large number of red cells are still hemolyzed (Figs. 6b, 7b).

Quantitatively, the results presented in the Fig. 8 show small values of the absorbance after 30 min in the case of untreated polymer surfaces, indicating that the blood clot is strongly linked. In this case, the small values of absorbance at 545 and 576 nm can be explained by the hemoglobin release through the lysis of the red cells situated on the clot external surface and its vicinity. In the case of the treated polymer surfaces this phenomenon appears to be prolonged. Even after 50 min of blood–surface contact a relatively high value of the hemoglobin absorbance is detected, proving that the coagulation process is not finished. This effect is more evident at the treated PET + TiO_2 surfaces (Fig. 8b).

The prolonged WBCT onto the treated surface has to be discussed in relation with the surface thermodynamic parameters, taking into account the role of plasma proteins in the adsorption at the surface. The generation of surfaces and interfaces that are able to reduce the protein adsorption is a major challenge in the use of anti-thrombogenic blood-contacting materials. Discussing the total forces implicated in the plasma proteins deposition and the creation of mechanically stable interfaces, Ruckenstein and Gourisankar [28] suggested that minimizing the interfacial tension between the blood and the material would allow obtaining biocompatible surfaces. Following their idea in explaining the effects of DBD treatments in the increase of WBCT, specific thermodynamic parameters, recognized for their key role in determining the hemocompatibility of surfaces of polymer implants, were calculated. Thus, the evaluation of the interfacial tension (γ_{SL}) between water, which represents more than 60% of the blood composition, and the polymeric surfaces showed that the DBD treatment induced a decrease of γ_{SL}, as shown in Table 7. The obtained values are approximately of the same magnitude as the interfacial energy between the cellular elements and the surface. This effect is in accord with the energetic criterion of Ruckenstein and Gourisankar [28]. The presence of TiO_2 in the matrix of the PET + TiO_2 sample is favorable for decreasing the values of the interfacial energy. Similar results were obtained for the polymer and plasma proteins (fibrinogen, immunoglobulin G—IgG and albumin) interface (Tables 8, 9) suggesting that DBD would be highly benefic in reducing the plasma proteins adsorption. Moreover, the decrease of the interfacial energy can stop the degradation of proteins structure and finally the activation of blood coagulation mechanism [28–30].

Table 7 Polymer-water interfacial energy (in mN/m)

Sample	Untreated	Treated
PET	29.22	1.60
PET + TiO_2	10.52	0.52

Table 8 PET—blood and PET—plasma proteins interfacial energy (in mN/m)

Biological liquids	Untreated PET	Treated PET
Blood	24.94	2.85
Fibrinogen	20.79	0.18
IgG	16.57	0.15
Albumin	15.04	0.34

Table 9 PET + TiO_2—blood and PET + TiO_2—plasma proteins interfacial energy (in mN/m)

Biological liquids	Untreated PET + TiO_2	Treated PET + TiO_2
Blood	7.72	2.08
Fibrinogen	5.85	0.06
IgG	4.14	0.68
Albumin	3.63	1.13

It is interesting to note that the order of adsorbed proteins amounts, derived from thermodynamic considerations, is changed after the DBD treatment. For the untreated surfaces the order of the adsorbed amount is albumin > IgG > fibrinogen, whereas the DBD treated samples present a reversed order, i.e. fibrinogen > IgG > albumin. Generally it is considered that the adsorption of albumin in high amounts would inactivate the blood–material interface, while a fibrinogen adsorbed in high amounts would favor the platelet adherence and the activation of the blood coagulation system. For the DBD treated samples, the small values of the interfacial energy between polymers and fibrinogen ensure low driving forces for protein deposition. Moreover, no structural changes in the fibrinogen structure are expected during adhesion. In this way, even though the fibrinogen is adsorbed preferentially onto the DBD treated polymer surfaces, the activation of the blood coagulation system is delayed. The stability of the interface could explain the prolonged whole blood coagulation times on the DBD treated samples.

Conclusions

The DBD treatment is an efficient tool, with low production costs, for the surface modifications of the PET and PET + TiO_2 films. After the DBD treatments the surfaces became rougher, presenting an increased effective surface area, the crystallinity degree and the crystallite size being also increased. The hydrophilic character of the samples was improved after the DBD treatments and, for long periods of storage in air, the treated samples remained more wettable than the untreated ones.

ATR-FTIR spectra showed no new adsorption bands, but the content of *trans* and *gauche* conformers in PET appeared to be modified, with a higher content of *trans* conformers, corresponding to the crystalline regions of PET found after the DBD treatment.

The blood formula in the presence of the samples showed no differences between untreated and treated polymer films.

The whole blood coagulation time was increased and the kinetics of coagulation for long periods of time was modified.

The DBD treated samples presented lower values of the interfacial energy with blood and plasma proteins, suggesting that DBD treatments represent an advantageous solution to minimize the blood-implants surface interfacial energy in accord with the Ruckenstein energetic criterion.

Acknowledgments The authors thank PhD Cristina Morariu, Hematology Laboratory, Military Hospital, Iasi, Romania, for its help with the hemocompatibility tests. This work was supported by the Romanian National University Research Council (CNCSIS) under Grant 1461/2005–2006.

References

1. Mao C, Qiu Y, Sang H, Mei H, Zhu A, Shen J, Lin S (2004) Adv Colloid Interface Sci 110(1–2):5
2. Chu PK, Chen JY, Wang LP, Huang N (2002) Mater Sci Eng R 36(5–6):143
3. Huang N, Yang P, Leng YX, Wang J, Sun H, Chen JY, Wan GJ (2004) Surf Coat Technol 186(1–2):218
4. Fridman G, Peddinghaus M, Balasubramanian M, Ayan H, Fridman A, Gutsol A, Brooks A (2006) Plasma Chem Plasma Process 26(4):425
5. Schroder K, Meyer-Plath A, Keller D, Besch W, Babucke G, Ohl A (2001) Contrib Plasma Phys 41(6):562
6. Wang J, Pan CJ, Huang N, Sun H, Yang P, Leng YX, Chen JY, Wan GJ, Chu PK (2005) Surf Coat Technol 196(1–3):307
7. Okazaki K, Nozaki T (2002) Pure Appl Chem 74(3):447
8. Dumitrascu N, Topala I, Popa G (2005) IEEE Trans Plasma Sci 33(5):1710
9. Visser SA, Hergenrother RW, Cooper SL (1996) In: Ratner BD, Hoffman AS, Schoen FS, Lemons JE (eds) Biomaterials science: an introduction to materials in medicine. Academic Press, San Diego, p 50
10. Pu FR, Williams RL, Markkula TK, Hunt JA (2002) Biomaterials 23(11):2411
11. Sanders JE, Bale SD, Neumann T (2002) J Biomed Mater Res 62(2):222
12. Zhang F, Zheng Z, Chen Y, Liu X, Chen A, Jiang Z (1998) J Biomed Mater Res 42(1):128
13. Strohm H, Sgraja M, Bertling J, Lobmann P (2003) J Mat Sci 38(8):1605
14. Pena J, Vallet-Regi M, San Roman J (1997) J Biomed Mater Res 35(1):129
15. Clark DT, Dilks A (1978) J Polym Sci Polym Chem Ed 16:911
16. Wu S (1982) Polymer interface and adhesion. Marcel Dekker, New York, p 184
17. Kwok SCH, Wang J, Chu PK (2005) Diamond Relat Mater 14(1):78
18. Agathopoulos S, Nikolopoulos P (1995) J Biomed Mater Res 29(4):421
19. Alexander LE (1969) X-ray diffraction methods in polymer science. Wiley Interscience, New York, p 335
20. Cole KC, Ajji A, Pellerin E (2002) Macromolecules 35(3):770
21. Koenig JL (1999) Spectroscopy of polymers. Elsevier, New York, p 90
22. Cenni E, Granchi D, Ciapetti G, Stea S, Verri E, Gamberini S, Gori A, Pizzoferrato A, Zucchelli P (1997) J Mater Sci Mater Med 8:771
23. Balakrishnan B, Kumar DS, Yoshida Y, Jayakrishnan A (2005) Biomaterials 26(17):3495
24. Fechine GJM, Souto-Maior RM, Rabello MS (2002) J Mater Sci 37(23):4979
25. Durell M, Macdonald JE, Trolley D, Wehrum A, Jukes PC, Jones RAL, Walker CJ, Brown S (2002) Europhys Lett 58(6):844
26. Lippert T (2005) Plasma Proc Polym 2(7):525
27. Chan CM, Ko TM, Hiraoka H (1996) Surf Sci Rep 24(1–2):1
28. Ruckenstein E, Gourisankar SV (1986) Biomaterials 7(6):403
29. Li ZF, Ruckenstein E (2004) J Colloid Interface Sci 269(1):62
30. Chen JY, Leng YX, Tian XB, Wang LP, Huang N, Chu PK, Yang P (2002) Biomaterials 23(12):2545